Optical Properties of Ho^{3+} Ions in Yttrium Gallium Garnet and Yttrium Iron Garnet

L. F. JOHNSON, J. F. DILLON, JR., AND J. P. REMEIKA
Bell Telephone Laboratories, Murray Hill, New Jersey 07974
(Received 28 August 1969)

Optical absorption and emission spectra are used to determine the energy levels of the $^5I_8$ ground state and $^5I_7$ excited state of Ho^{3+} in diamagnetic yttrium gallium garnet (YGaG) and ferrimagnetic yttrium iron garnet (YIG). The results for YGaG are consistent with the D_2 site symmetry of the dodecahedral site in the garnet structure. Energy levels in YIG which are separated by site inequivalency are identified from spectra observed as the Fe^{3+} magnetization is rotated in the $(1\bar{1}0)$ plane. Stimulated emission is observed from Ho^{3+} in YGaG at 2.086 and 2.114 μ and from Ho^{3+} in YIG at 2.086, 2.089, and 2.107 μ. Each of the lines in YIG is composed of two superimposed electronic transitions. The exchange field in YIG makes possible magnetic tuning of coherent emission over a range of 70 Å.

INTRODUCTION

THE discovery of a highly transparent window in the near infrared in ferrimagnetic yttrium iron garnet (YIG),[1,2] combined with the knowledge that several trivalent rare-earth ions fluoresce strongly within this window, has resulted recently in the observation of stimulated emission from Ho^{3+} ions in YIG.[3] The magnetic nature of YIG offers the prospect of being able to substantially alter the coherent output through a host of magneto-optical schemes.

This paper presents experimental data on the spectroscopy of Ho^{3+} in YIG and its diamagnetic counterpart, yttrium gallium garnet (YGaG). The results are used to construct energy-level diagrams for the ground state $^5I_8$ and the first excited state $^5I_7$ and to ascertain the energy levels involved in optical maser transitions. Energy levels in YIG which are separated by site inequivalency are identified from spectra observed as the Fe^{3+} magnetization **M** is rotated in a {110} plane. The anisotropic splitting makes possible magnetic tuning of coherent emission over a range of 70 Å. Other data pertinent to optical maser operation, such as energy transfer and fluorescence lifetime, are also presented.

A thorough study of the energy levels of the Ho^{3+} ion in $LaCl_3$ has been made by Dieke and Pandey,[4] and the energy levels in ethylsulfate have been studied in absorption by Grohmann *et al.*[5] Levels of the lowest two manifolds in yttrium aluminum garnet also have been reported.[6] Previous spectroscopic studies of the rare-earth–iron exchange interaction in iron garnet include the detailed study of ytterbium in YIG in which exchange splittings were deduced from the anisotropic behavior of the transition between the lowest level of the ground state and the lowest level of the excited state as the iron magnetization was rotated in a {110} plane.[7] Dillon and Walker[8] calculated the effect of exchange on the levels of the ground manifold of terbium in YIG to explain anomalies in the frequency of ferrimagnetic resonance.

We shall be concerned primarily with optical transitions between the two lowest manifolds $^5I_8$ and $^5I_7$ of Ho^{3+} in YGaG and YIG.

EXPERIMENTAL

The YGaG and YIG crystals were grown from melts contained in platinum crucibles. Growth was achieved by slow cooling and self-nucleation after the constituent oxides were dissolved in a $PbO(B_2O_3)_x$ flux system at 1300°C. Emission spectroscopic analysis of the starting materials showed <10 ppm of Si and Ca, the highest impurity levels found. The Y_2O_3 and Ho_2O_3 were further examined by mass spectrographic analysis. Total rare-earth impurity content was well below 2 ppm.

Absorption data with no magnetic field was obtained with a Cary Model 14 spectrophotometer. Spectra of YGaG:Ho^{3+} were recorded at 2 and 20°K over the range 0.4–2.5 μ. The 2°K spectra for Ho^{3+} concentrations of 2 and 7% were identical. Data on YIG:Ho^{3+} was obtained at 2, 20, and 77°K from 1 to 2.5 μ for Ho^{3+} concentrations of 1 and 3%. The variations of absorption to the $^5I_7$ first excited state of Ho^{3+} in YIG with the direction of the Fe^{3+} sublattice magnetization **M** was observed with a 50-W tungsten lamp, a Perkin-Elmer 112-G grating spectrometer, and a PbS detector. The samples, prepared as sections parallel to $(1\bar{1}0)$ faces, were immersed in liquid helium, and a horizontal field of 17 000 G was applied in the plane of the section. The orientation of **M** was changed by rotating the samples in 2.5° increments about the normal to the major faces.

Fluorescence of YGaG:Ho^{3+} was excited by an Osram 200-W Hg lamp with a water filter. The mercury lamp was not suitable for YIG:Ho^{3+} at low temperature, since absorption in the Fe^{3+} absorption band

[1] J. F. Dillon, Jr., J. Phys. Radium **20**, 374 (1959).
[2] R. C. LeCraw, D. L. Wood, J. F. Dillon, Jr., and J. P. Remeika, Appl. Phys. Letters **7**, 27 (1965).
[3] L. F. Johnson, J. P. Remeika, and J. F. Dillon, Jr., Phys. Letters **21**, 37 (1966).
[4] G. H. Dieke and B. Pandey, J. Chem. Phys. **41**, 1952 (1964).
[5] I. Grohmann, K. H. Hellwege, and H. G. Kahle, Z. Physik **164**, 243 (1961).
[6] L. F. Johnson, J. E. Geusic, and L. G. Van Uitert, Appl. Phys. Letters **8**, 200 (1966).
[7] K. A. Wickersheim and R. L. White, Phys. Rev. Letters **4**, 123 (1960); K. A. Wickersheim, Phys. Rev. **122**, 1376 (1961); K. A. Wickersheim and R. L. White, Phys. Rev. Letters **8**, 483 (1962).
[8] J. F. Dillon, Jr., and L. R. Walker, Phys. Rev. **124**, 1401 (1961).

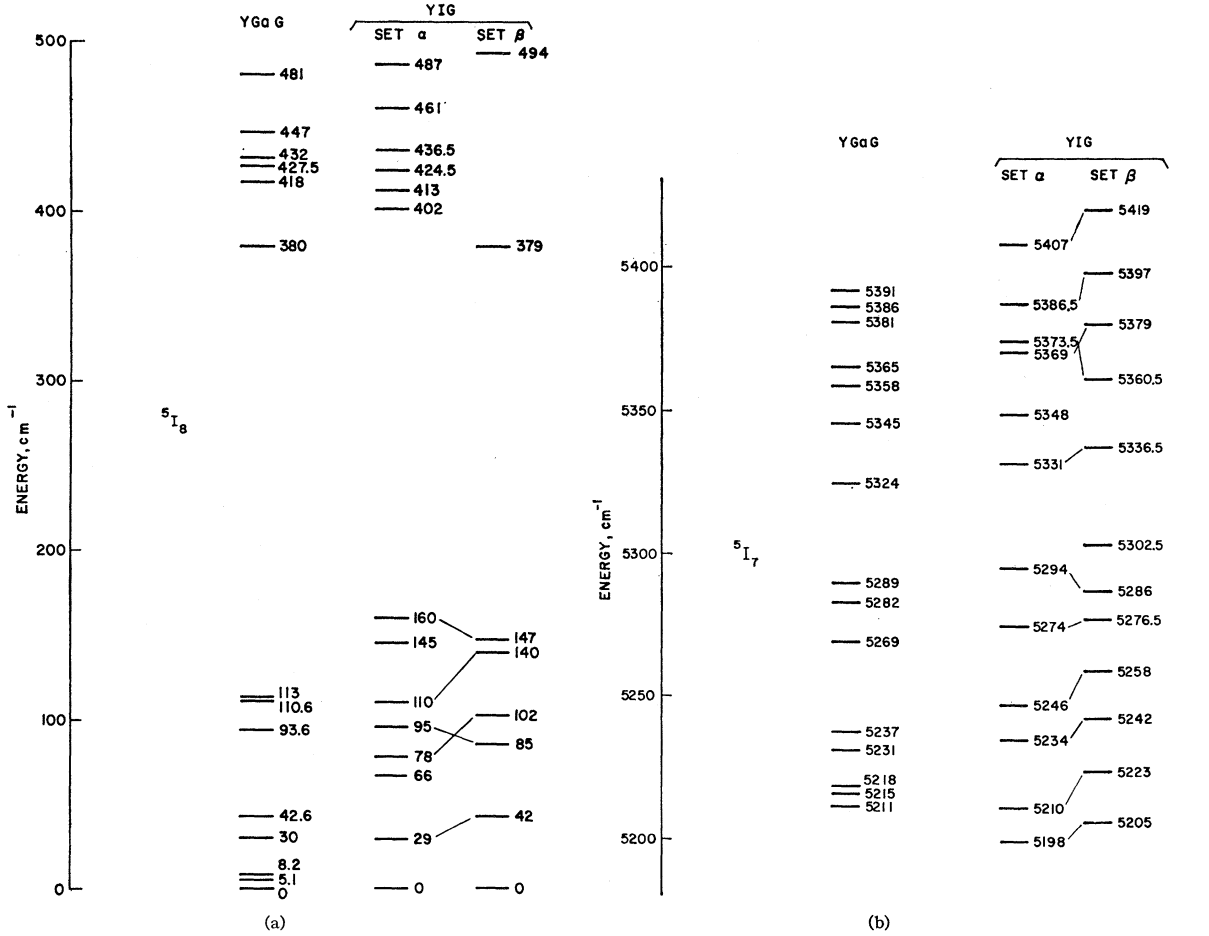

FIG. 1. (a) Energy levels of $^5I_8$ ground state of Ho^{3+} in YGaG and YIG. (b) Energy levels of $^5I_7$ excited state of Ho^{3+} in YGaG and YIG.

below 1 μ produced excessive heating of the crystal. Excitation was provided by a Sylvania CZA 500-W tungsten lamp with appropriate filters. The filters consisted of a silicon window together with multilayer dielectric coated glass slides having high transmission in the near infrared but with less than 0.1% transmission in the region of Ho^{3+} fluorescence between 1.9 and 2.2 μ. The variation of emission with direction of **M** at 4.2°K was observed in the Varian magnet. Data at 77°K were obtained with a magnetron magnet (field $\sim$3000 G).

Excitation spectra were obtained by monitoring the strength of Ho^{3+} emission as the exciting radiation from a type DXN 1000-W tungsten lamp was scanned through the visible and near infrared by means of the 112-G grating spectrometer. A germanium filter prevented pump light from reaching the monitoring PbS detector.

Initial pulsed optical maser experiments were carried out at 77°K in an FT524 helical xenon lamp. The output was directed onto a cooled Au-doped germanium detector after being dispersed by a grating spectrometer. The arrangement for obtaining magnetic tuning of coherent emission from YIG:Ho^{3+} consisted of placing the maser crystal and an FT90 linear xenon flash lamp at the foci of a cylindrical ellipse reflector with the entire assembly mounted in the 6-in. gap of an electromagnet (2800 G). The crystal was cooled to about 85°K by immersion in a circulating stream of precooled liquid oxygen. The axis of the maser rod corresponded to a ⟨110⟩ crystallographic direction and tuning was achieved by simply rotating the crystal about this axis normal to the direction of the magnetic field.

ENERGY LEVELS OF Ho^{3+} IN YGaG

At 2°K there are 18 lines observed in absorption from $^5I_8$ to $^5I_7$. Four of these are temperature-dependent in intensity and separated by 5.1 cm^{-1} from adjacent lines at higher energy. These lines locate an excited level of the ground manifold at 5.1 cm^{-1}. Thirteen lines are temperature-independent and establish 13 levels of the $^5I_7$ excited state [Fig. 1(b)]. The remaining line in absorption at 5375.5 cm^{-1} has the same temper-

ature dependence as the other four, but an adjacent line higher in energy by 5.1 cm^{-1} is too weak to be seen clearly. Therefore, the level at 5380.6 cm^{-1} is inferred on the basis of the temperature-dependent line at 5375.5 cm^{-1}. An additional level is assigned to the excited state at 5215.4 cm^{-1} based on four temperature-dependent emission lines (2 and 4.2°K) and two additional lines seen in absorption at 20°K. Thus, the 15-fold degeneracy of the excited state is completely removed by the crystal field, as expected for the D_2 site symmetry of the dodecahedral site in the garnet structure. Using the formula

$$f=\frac{mc^2}{\pi e^2}\frac{1}{n}\int \sigma d\nu, \qquad (1)$$

where σ is the absorption cross section (cm^2), ν is the frequency (cm^{-1}), $n\simeq 1.9$ is the index of refraction, and the other symbols have their usual meanings. The oscillator strength f of transitions to $^5I_7$ from the lowest level of the ground state are given in Table I. Assignments for these transitions and a comparison of calculated and observed oscillator strengths have been made by Kamimura and Yamaguchi.[9]

The levels of the $^5I_8$ ground manifold are determined mainly from fluorescence data at 2 and 4.2°K (Fig. 2). The first line in absorption at 2°K coincides with the highest energy line in emission (5210.8 cm^{-1}) so that 14 of the 17 levels of $^5I_8$ are found by simply subtracting the frequency of the various emission lines from 5210.8 cm^{-1} [Fig. 1(a)]. It will be noted that transitions to the higher-lying levels of $^5I_8$ are very broad (Fig. 2). Transitions to the three remaining levels are believed to lie in this region. The levels at 5, 8, 30, and 43 cm^{-1} are confirmed by absorption at 20°K.

Transitions to some of the low-lying levels of the ground state have been seen in absorption in the far infrared.[10] Lines are seen in HoGaG at 26.5, 30.3, 39.0, 44.2, 86, and 111 cm^{-1}. The lines at 30.3, 44.2, and 111 cm^{-1} agree fairly well with our assignments for the single ion while the remaining lines may represent pair lines, etc.

TABLE I. The oscillator strength of transitions to $^5I_7$ from the lowest level of the ground state of Ho^{3+} in YGaG (2°K).

Frequency (cm^{-1})	Assignment[a] $^5I_8 \rightarrow {}^5I_7$	Oscillator strength f (units of 10^{-8})
5210.8	$A_2 \rightarrow A_2$	2.6
5214.8	$\rightarrow B_2$	...
5218.1	$\rightarrow B_1$	2.1
5230.9	$\rightarrow A_1$	2.3
5237.2	$\rightarrow B_2$	0.3
5268.7	$\rightarrow B_1$	2.6
5282.3	$\rightarrow A_2$	1.5
5289	$\rightarrow B_1$	0.3
5324	$\rightarrow B_2$	<0.07
5345.3	$\rightarrow A_1$	1.3
5358.2	$\rightarrow A_2$	9.8
5364.8	$\rightarrow A_1$	3.6
5380.6	$\rightarrow A_2$	...
5385.9	$\rightarrow B_2$	6.4
5391.4	$\rightarrow B_1$	1.4

[a] From Ref. 9.

[9] H. Kamimura and Y. Yamaguchi, Phys. Rev. (to be published).

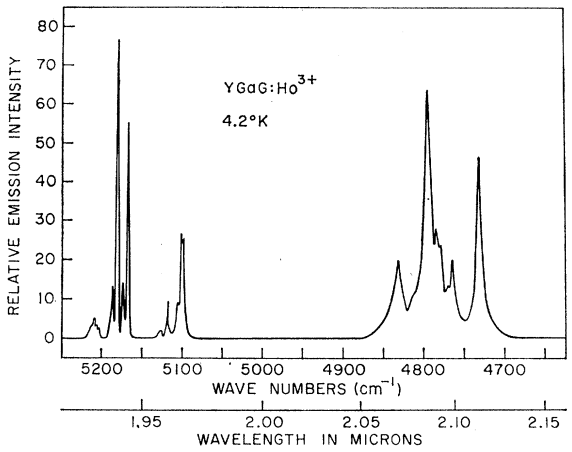

FIG. 2. $^5I_7 \rightarrow {}^5I_8$ emission spectrum of Ho^{3+} in YGaG at 4.2°K.

ENERGY LEVELS OF Ho^{3+} IN YIG

The task of sorting out the energy levels of Ho^{3+} in YIG is not trivial. It will be recalled that the symmetry of the crystal field in YGaG is sufficiently low that all energy-level degeneracy in the Ho^{3+} ion is removed, leaving 15 levels in the excited state and 17

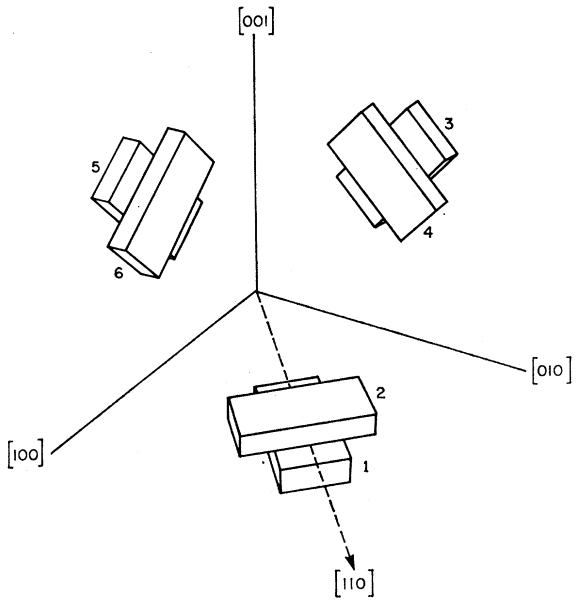

FIG. 3. Diagram of the spatial orientation of the six magnetically inequivalent dodecahedral sites for a rare-earth ion in YIG (from Dillon and Walker, Ref. 8).

[10] A. J. Siever, III, and M. Tinkham, Phys. Rev. 129, 1995 (1963).

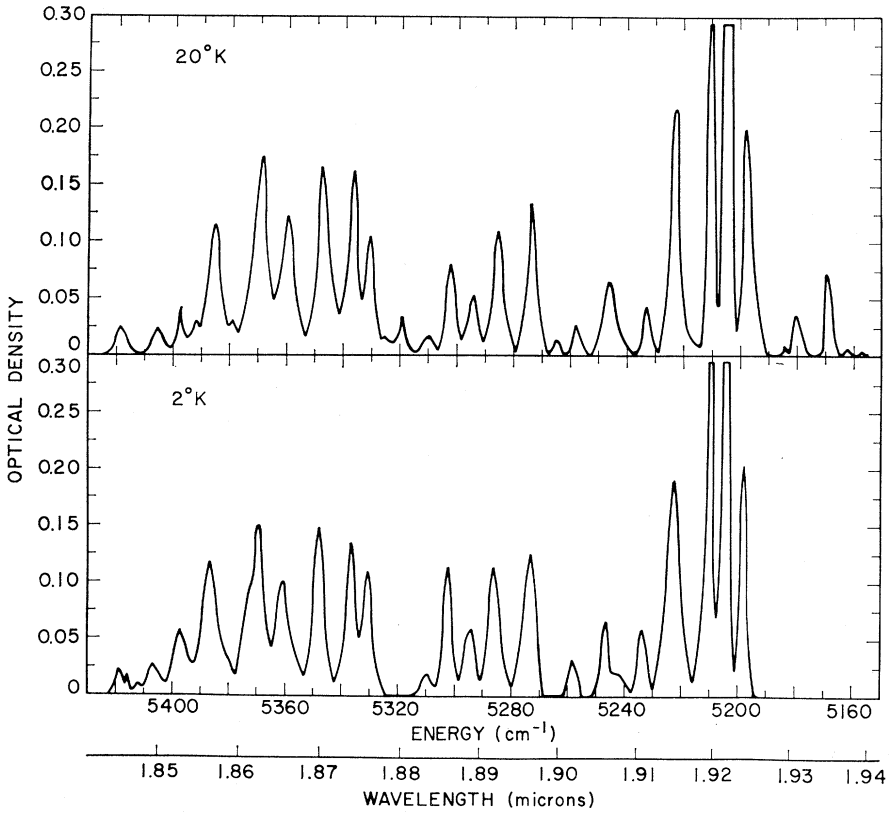

FIG. 4. $^5I_8 \rightarrow {}^5I_7$ absorption spectrum of Ho^{3+} (1%) in YIG at 2 and 20°K. Crystal thickness 1.75 mm.

levels in the ground state. In the case of YIG, one has the additional influence of a very large exchange field produced by the Fe^{3+} spins. A convenient way of visualizing the six magnetically inequivalent sites in the garnet lattice and their relative orientation is provided by the matchbox diagram of Dillon and Walker[8] shown in Fig. 3. The disposition of the three twofold axes of the D_2 sites is shown by the orientation of the matchboxes. If the magnetization is along a general direction, all of these sites are inequivalent. However, for the magnetization in certain symmetry planes and directions, the number of inequivalent sites is reduced. For example, as **M** swings around the $(1\bar{1}0)$ plane from [001] to [110], sites 3 and 5 are always equivalent and 4 and 6 are always equivalent. For **M** along [001], sites 1 and 2 are degenerate, as are 3, 4, 5, and 6. In contrast for **M** along [110], sites 1 and 2 are *inequivalent*, while 3, 4, 5, and 6 are equivalent. When **M** becomes parallel to [111], the rare-earth sites are divided into two sets; 1, 3, and 5 are distinct from 2, 4, and 6. This last case is of added importance because the easy directions of magnetization in YIG are ⟨111⟩ axes, and in the absence of a field almost all of the magnetization lies along the easy axes. These changing degeneracies are immensely useful in the site assignment of many optical transitions.

Starting from absorption and emission spectra at 2°K in zero magnetic field, the problem consists of assigning each line to either one or the other of the two sets of sites present for $H=0$. About 35 levels can be assigned with some certainty on the basis of additional lines appearing in spectra at 20°K. A few levels are assigned or confirmed from lines appearing at 77°K. Where possible, the dependence of line strength on temperature is used to select or discard a possible assignment. Some absorption and emission lines are found to be temperature-dependent as a result of the superposition of other lines—behavior which is particularly relevant with regard to the optical maser transitions. Finally, several assignments are made from splittings apparent in the spectra as the magnetization is rotated in a {110} plane.

At ~2°K, with no magnetic field, there are two lines which are coincident in absorption and emission [Figs. 4 and 5(a)]. These identify lowest levels of the $^5I_7$ manifold at 5198 and 5205 cm^{-1} for the two sets of sites (call them α for sites 1, 3, and 5 and β for sites 2, 4, and 6) existing in the field-free case. There are 12 additional lines in emission at 20°K [Fig. 5(b)] which are spaced about 12 cm^{-1} to higher energy from adjacent lines present at 2°K. There is also an absorption line at 5210 cm^{-1} at 2°K and, therefore, we assign this higher-lying emitting state at 5210 cm^{-1} to set α.[11] More importantly, this identifies 12 levels of the $^5I_8$

[11] If the level at 5210 cm^{-1} belonged to set β, it would lie only 5 cm^{-1} above the lowest $^5I_7$ level of set β and the 11 additional emission lines present at 20°K should also be seen at 4.2°K, contrary to what is observed.

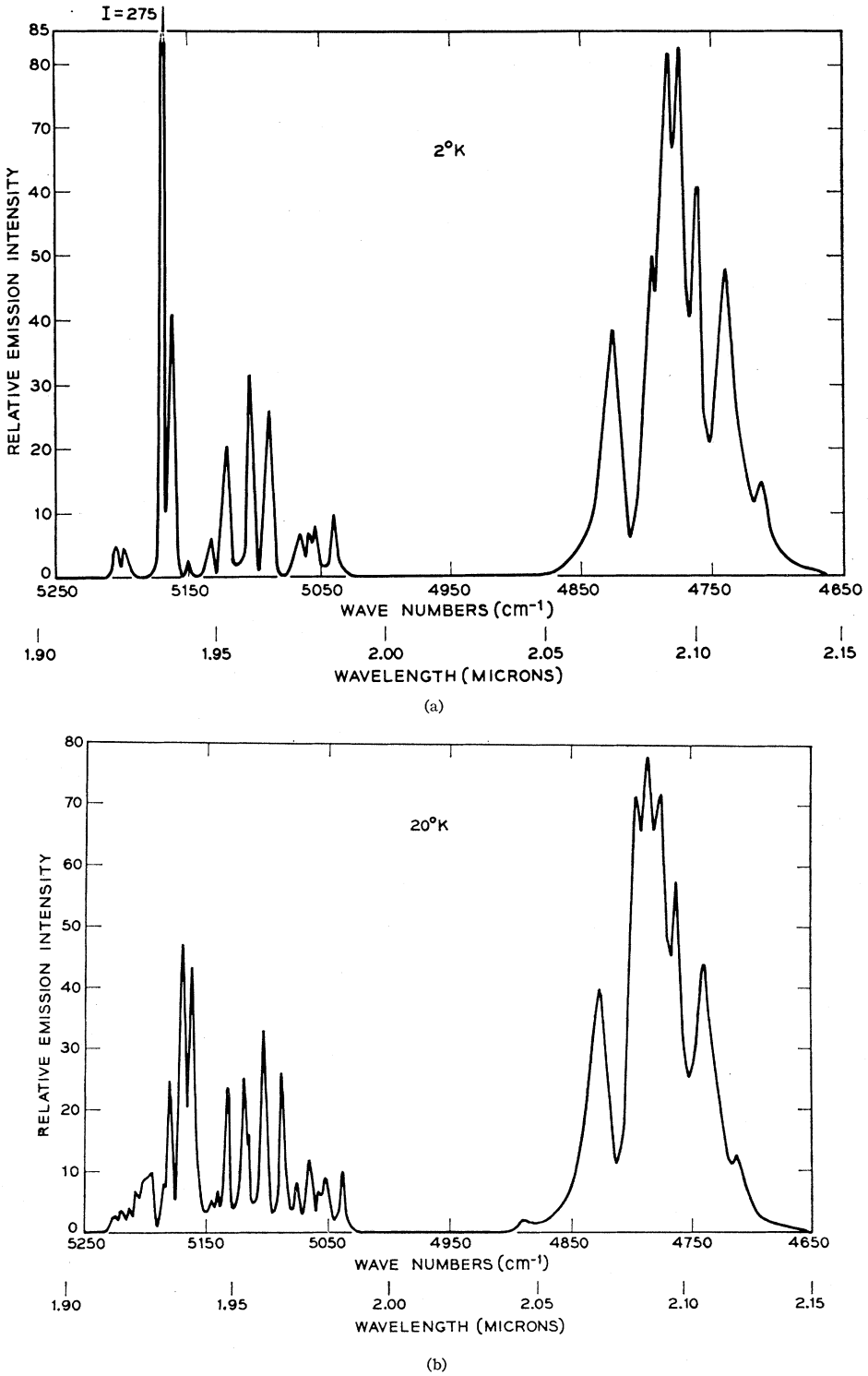

FIG. 5. (a) $^5I_7 \rightarrow {}^5I_8$ emission of Ho^{3+} in YIG at 2°K. (b) $^5I_7 \rightarrow {}^5I_8$ emission of Ho^{3+} in YIG at 20°K.

ground manifold of set α, located at 0, 29, 66, 78, 95, 145, 160, 402, 413, 424.5, 436.5, and 461 cm^{-1} [Figs. 1(a) and 1(b)]. Similarly, there are 4 additional lines in emission at 20°K spaced about 18 cm^{-1} to higher energy from adjacent lines present at 2°K. Since there is a 2°K absorption line at 5223 cm^{-1} (18 cm^{-1} above the 5205 cm^{-1} emitting state of set β) we assign a higher-lying β emitting state at 5223 cm^{-1}, while the additional emission lines establish ground manifold levels for set β at 0, 140, 147, 379, and 494 cm^{-1} [Figs. 1(a) and 1(b)].

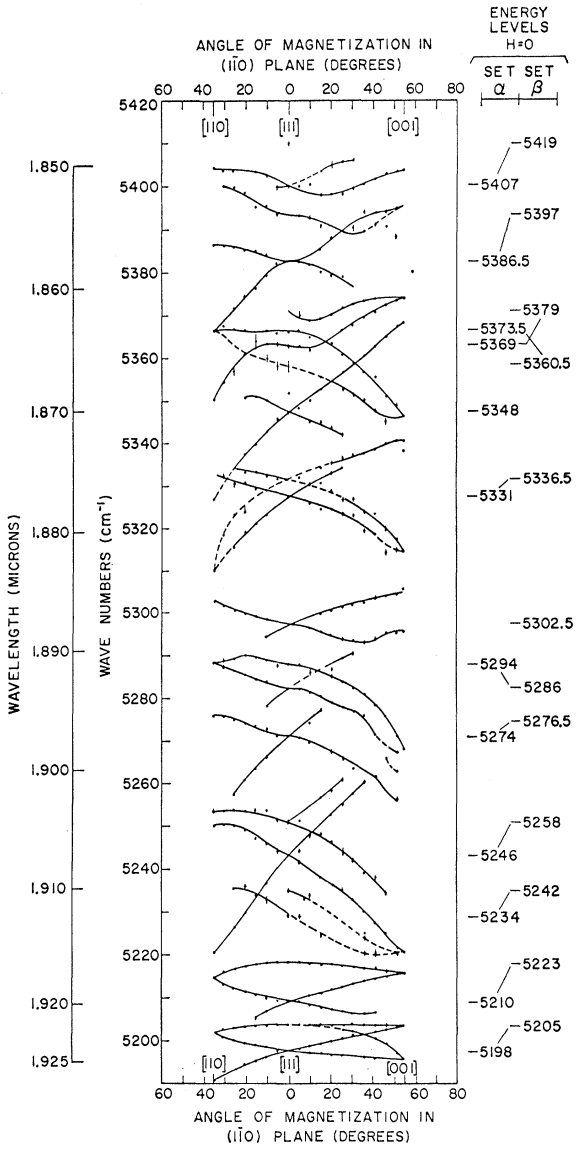

FIG. 6. Variation of $^5I_8 \rightarrow {}^5I_7$ absorption lines of Ho^{3+} in YIG as the magnetization is rotated in the (1$\bar{1}$0) plane. The numbers opposite frequencies for H along [111] indicate α and β levels in zero magnetic field.

In absorption at 20°K (Fig. 4), there are 8 lines spaced 29 cm^{-1} to lower energy from adjacent lines seen at 2°K. These confirm α levels at 29 and 5210 cm^{-1} and locate additional α levels in the excited state at at 5234, 5246, 5274, 5294, 5331, and 5348 cm^{-1}. Emission from 5234 cm^{-1} at 20°K identifies α levels at 110 and 487 cm^{-1} and confirms α levels at 78 and 95 cm^{-1}. Two absorption lines at 77°K from the α level at 66 cm^{-1} support the assignment of α levels at 5331, 5348, 5373.5, and 5407 cm^{-1}.

In absorption at 20°K, there are 2 lines separated by 42 cm^{-1} to lower energy from β lines at 5205 and 5223 cm^{-1}. These establish a β level at 42 cm^{-1}. Three additional 42 cm^{-1} differences assign β levels at 5258, 5360.5, and 5419 cm^{-1}. Emission from 5258 cm^{-1} at 20 and 77°K supports β levels at 85 and 102 cm^{-1}, and absorption from 85 cm^{-1} at 77°K assigns β levels at 5242, 5276.5, and 5336.5 cm^{-1}. Absorption lines from the level at 147 cm^{-1} at 77°K are believed to identify β levels at 5286 and 5302.5 cm^{-1}.

We next consider the behavior of the $^5I_8 \leftrightarrow {}^5I_7$ transition frequencies as the magnetization **M** is rotated in the (1$\bar{1}$0) plane by a magnetic field of 17 000 G. At 4.2°K, a field of 17 000 G is not sufficient to overcome the magnetic anisotropy and move the magnetization to the [110] and [001] directions. However, ferrimagnetic resonance data on Ho^{3+} in YIG[12] suggests that the anisotropy decreases rapidly with increasing temperature. Therefore, in addition to measurements at 4.2°K, absorption and fluorescence data were also obtained at 20°K.[13] The splittings observed at 20°K as the external field deviated from the [110] and [001] directions (which were markedly different from those appearing at 4.2°K) confirmed that the magnetization direction was controlled by the field except for angles very close to [001].[14] Hence, the 20°K data was necessary for observing the true behavior of optical transitions in the vicinity of the hard [110] and [001] directions, and Figs. 6 and 7 represent a composite of both sets of data.

When H is along [111], absorption and emission spectra at 4.2 and 20°K are identical, except for additional lines appearing at 20°K. However, an external field of 17 000 G along [111] produces a significant shift of the transition frequencies (as much as 6 cm^{-1}) from their zero-field values. Except for transitions between the lowest levels of the ground and excited states, which are essentially unchanged, the applied field has the effect of lowering the energy levels of both the ground state and the excited state from their zero-field positions. The shifts are such that the splittings between corresponding energy levels in sets α and β are reduced, indicating that the applied field and the exchange field are antiparallel. In Figs. 6 and 7, the zero-field α and β energy levels are listed opposite their corresponding locations for H along [111] to permit an estimate of the shifts from the zero-field positions as well as to correlate the magnetic behavior of the optical transitions with the electronic states involved.

The following information can be obtained from the data in Figs. 6 and 7: Energy levels previously assigned to set α or β on the basis of zero-field data can be confirmed; levels for which insufficient information is available in the zero-field spectra can be immediately

[12] J. F. Dillon, Jr., and J. W. Nielsen, Phys. Rev. **120**, 105 (1960).
[13] Care must be exercised in interpreting the 20°K data since there are nearly twice as many lines appearing at 20°K as at 4.2°K.
[14] A comparison with the 20°K data revealed that at 4.2°K the magnetization lagged the 17 000-G field by about 10° when H is directed along [110] or [001].

assigned to set α or β; each energy level of set β can be identified with its corresponding component in set α and the splitting due to site inequivalency can be deduced. As stated earlier, the exchange field divides the Ho^{3+} ions into two inequivalent sets of sites: α representing sites 1, 3, and 5 and β with sites 2, 4, and 6. When an external magnetic field swings the Fe^{3+} magnetization to an [001] direction, sites 1 and 2 (and also 3 and 4) become degenerate. Hence, corresponding levels in α and β can be recognized by degeneracy when **M** is along [001]. It is readily apparent, for example, that the lowest excited state level of α at 5198 cm^{-1} is split by the exchange field from the lowest excited state level of β at 5205 cm^{-1}. Other level correspondences between α and β are indicated by connecting lines between zero-field levels. Furthermore, sites 3 and 4 are distinguished from sites 1 and 2 if degeneracy exists for **M** along [110] as well as along [001]. This distinction can be seen most clearly in the absorption and emission lines near 5200 cm^{-1} and the emission lines near 5170 cm^{-1}. In the case of the transition between the lowest level of the ground and excited state, a complete classification of lines according to sites can be made by comparison with theory.[9] For **M** at, say, 45° from [111] toward [001], the absorption lines near 5200 cm^{-1} can be labeled in the order of increasing energy as belonging to sites 3, 4, 1, and 2.

Since each energy level in set α corresponds to one in set β split by site inequivalency, the data in Figs. 6 and 7 serve as a check on the correctness of level assignments into sets α and β from spectra in zero magnetic field. In all cases in which this test can be made, the assignments are confirmed. In addition, several levels for which the data in zero field is insufficient to make an assignment can be identified. The levels seen in absorption in zero field at 5369 and 5379 cm^{-1} are obviously split by inequivalency, as well as the levels at 5386.5 and 5397 cm^{-1}. Examination of theoretical curves[9] shows that an α transition from the lowest level of the ground state to a level of the excited state lies lower in energy than the corresponding transition in set β. Therefore, the lower level of each of the above pair is assigned to α. We must point out, however, that theory and experiment are in only fair agreement; for instance, two β levels at 5286 and 5360.5 cm^{-1} lie lower on the basis of experimental data than their corresponding levels in α at 5294 and 5373.5 cm^{-1}.

The zero-field oscillator strength of α and β transitions to $^5I_7$ from the lowest level of the ground state are listed in Table II.

Several disappointing aspects of the experimental results should be mentioned. First of all, only 14 of the 17 levels of the $^5I_8$ ground manifold of α and 8 levels of β have been found, and only 12 of the 15 levels in the excited state of α and β have been identified. From the spectra at 2 and 20°K, only one weak absorption line

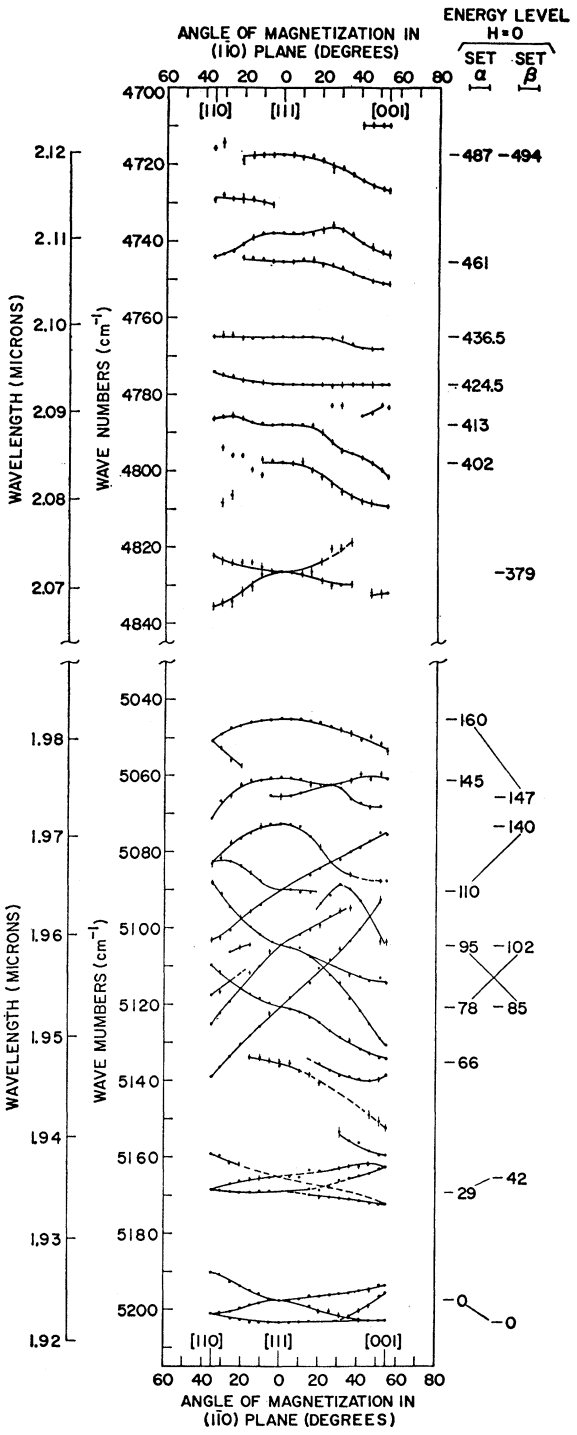

FIG. 7. Variation of $^5I_7 \rightarrow {}^5I_8$ emission lines of Ho^{3+} in YIG as the magnetization is rotated in the (1$\bar{1}$0) plane. The numbers opposite frequencies for H along [111] indicate α and β levels derived from emission lines in zero field.

(2°K) at 5310 cm^{-1} and a weak line at 5184 cm^{-1} at 20°K (seen in both absorption and emission) have not been assigned. Second, it is difficult to follow many

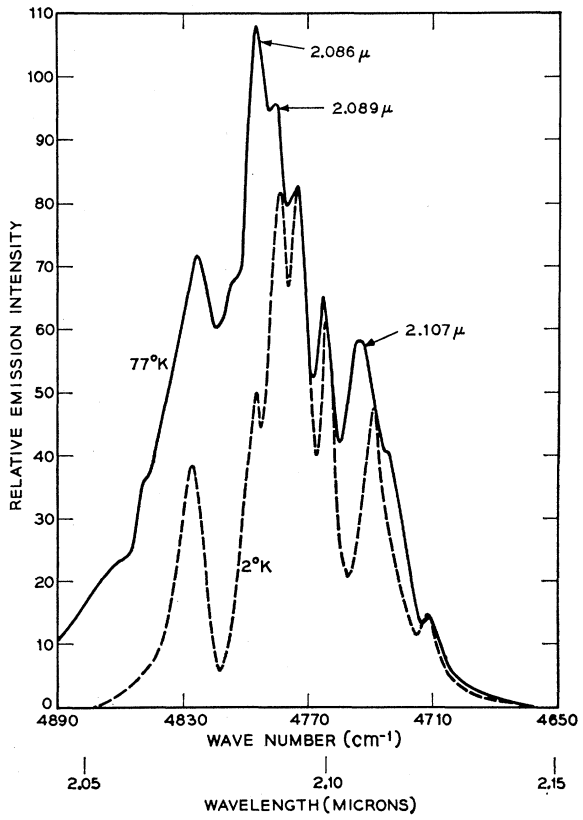

FIG. 8. Fluorescence in region of maser transitions at 2 and 77°K. Maser lines are indicated by arrows.

lines as **M** is rotated in the $(1\bar{1}0)$ plane, either because of overlap with other lines or diminishing intensity. For only two transitions is it possible to observe all four inequivalent sites for an arbitrary direction of **M** in the $(1\bar{1}0)$ plane. Failure to obtain a thorough mapping of most if not all transitions for the four sites renders a complete comparison with the theory of Kamimura and Yamaguchi very uncertain.

Finally, in the far-infrared spectrum of Ho (5%) in YIG,[10] absorption lines have been seen at 22.1, 29.4, 43.5, 66.5, and 83.5 cm^{-1}. The lines at 29.4, 43.5, 66.5, and 83.5 cm^{-1} are explained by our α and β identification for these levels for the field-free case. The line at 22.1 cm^{-1} is unaccounted for.

OPTICAL MASER EXPERIMENTS

A. Optical Maser Transitions

At 77°K, coherent oscillation is observed from Ho^{3+} in YGaG in two lines at 2.086 and 2.114 μ, with pulse thresholds of 70 and 250 J, respectively, into an FT 524 xenon lamp. The lines correspond to transitions from the lowest level of the excited state at 5211 cm^{-1} to levels of the ground state at 418 and 481 cm^{-1}, respectively [see Figs. 1(a) and 1(b)].

In YIG:Ho^{3+}, coherent emission is observed in three lines (A, B, and C) at 77°K. Line A at 2.086 μ (4794 cm^{-1}) corresponds to a transition from the lowest level of the $^5I_7$ excited state of set α at 5198 cm^{-1} to the $^5I_8$ ground manifold level at 402 cm^{-1} [Figs. 1(a) and 1(b)]. Similarly, line B at 2.089 μ (4787 cm^{-1}) consists primarily of α emission from 5198 to 413 cm^{-1}. However, both of these lines in fluorescence are strengthened at 20°K and higher temperatures (Fig. 8) by the superposition of transitions from the α level at 5210 cm^{-1}: line A by a transition to 413 cm^{-1} and line B by the transition to 424.5 cm^{-1} (Fig. 9). Line C at 2.107 (4746 cm^{-1}) is not observed in fluorescence at 2°K (Fig. 8); it represents an α transition from a higher-lying $^5I_7$ level at 5234 cm^{-1} to the ground manifold level at 487 cm^{-1}. At 20°K it appears as a weak shoulder on a broad α transition 5198 to 461 cm^{-1}; at 77°K, it is dominant. The frequency of maser line C at 77°K is determined by the maximum of the gain profile for these two overlapping lines. Thus, at 77°K, each of the maser lines is composed of a pair of Ho^{3+} transitions.

The threshold of line C is very sensitive to temperature in the region of 80°K. While the thresholds for lines A and B increase by ~10–20% between 77 and 90°K, the threshold of line C decreases drastically. This

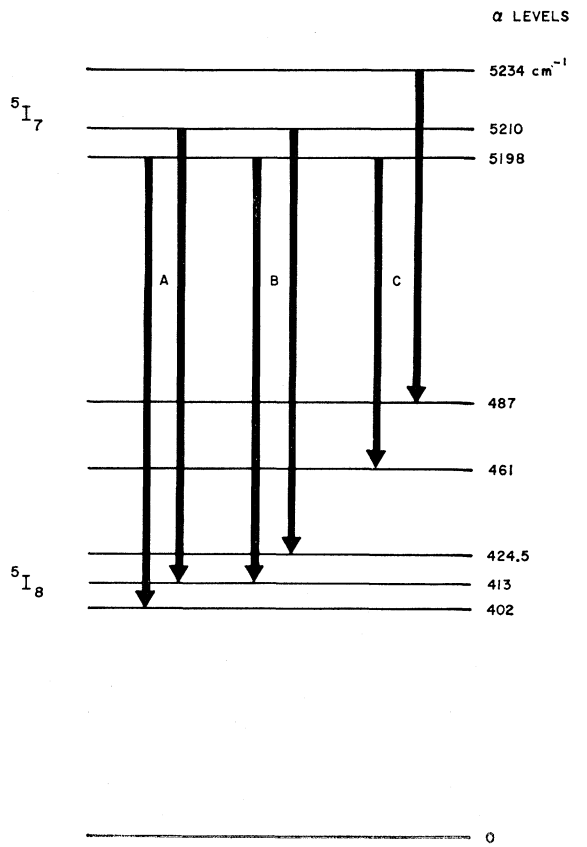

FIG. 9. Ho^{3+} energy-level diagram showing the α transitions involved in the three maser lines.

behavior is consistent with the observation that much of the strength of line C is acquired through thermal population of the 5234 cm^{-1} state lying 36 cm^{-1} above the lowest α level of $^5I_7$.

B. Considerations on Continuous Maser Oscillation from Ho^{3+} in YIG

Under pulse illumination in an FT524 xenon lamp, the lowest pulse thresholds observed for Ho^{3+} in YIG at 77°K are 30 J for lines A and B and 50 J for line C (12-μF storage condenser). The measurements were made on crystals in which 5% erbium, 5% thulium (energy-transfer ions), and 2% holmium were substituted for yttrium. Since the fluorescence lifetime of Ho^{3+} in YIG at 77°K is 3.6 millisec, conditions are quite favorable for continuous maser oscillation. An idea of what should be achieved can be obtained by a comparison with Ho^{3+} in YAG.[6] The fluorescence lifetime of Ho^{3+} in YAG is 6.6 millisec at 77°K, which we take to reflect a higher fluorescence quantum efficiency. Since radiation below 1 μ must be rejected for YIG:Ho^{3+}, the effective pumping efficiency under tungsten lamp illumination is about 20% for YIG:Ho^{3+} and 60% for YAG:Ho^{3+}, both containing Er^{3+} and Tm^{3+} ions for energy transfer. However, a greater fraction of the energy absorbed by YAG:Ho^{3+} is dissipated in nonradiative decay to the metastable state. Taking into account that the fluorescence linewidth is somewhat broader in YIG and the fraction of the total emission occurring in the maser transition somewhat less than

TABLE II. The zero-field oscillator strength of α and β transitions to $^5I_7$ from the lowest level of the ground state of Ho^{3+} in YIG (2°K).

Frequency (cm^{-1})		Oscillator strength f[a] (units of 10^{-8})	
α	β	α	β
5198.2		2.2	
	5205.1		5.6
5210		4.7	
	5222.8		3.6
5234		1.2	
	5241.6		0.4
5246.3		1.0	
	5258.2		7.3
5273.7		2.2	
	5276.5		0.7
	5286.2		2.2
5294.1		1.4	
	5302.5		1.8
5330.8		2.0	
	5336.5		3.2
5347.9		2.8	
	5360.5		2.8
5369.4		4.2	
5373.5		1.6	
	5379.2		0.3
5386.5		3.9	
	5397.2		1.4
5406.9		0.8	
	5418.9		0.6

[a] A value of $n=2.195$ at 2 μ is used for the refractive index in Eq. (1) [C. R. Staton (unpublished)].

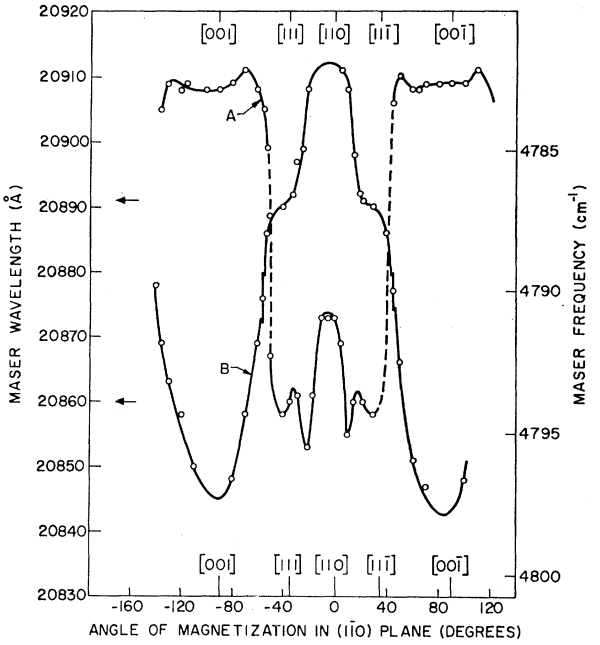

FIG. 10. Tuning of maser lines A and B by rotation of the magnetization in the (1$\bar{1}$0) plane. The arrows pointing to the left indicate the maser wavelengths in zero magnetic field.

in YAG, we estimate that the cw threshold of YIG:Ho^{3+} should be a factor of 5 or 6 higher than for YAG:Ho^{3+}. cw oscillation was attempted in a cylindrical ellipse pumping configuration with a 500-W T3Q tungsten lamp at one focus and the maser crystal at the other. A polished silicon slab, placed between lamp and crystal, eliminated radiation in the region of Fe^{3+} absorption below 1.1 μ. The silicon was antireflection coated with silicon monoxide to provide a transmission of >90% in the effective pumping range from about 1.2 to 2.0 μ.[15] A circulating stream of precooled liquid nitrogen cooled the crystal to about 70°K. The polished ends of the crystal rods were coated with multilayer dielectric reflectors with transmissions of 0.1 and 0.4% at 2.1 μ.[16] Although the cw threshold for a rod of Ho^{3+} in YAG was reached with 45 W into the lamp, cw oscillation of YIG:Ho^{3+} could not be obtained at 600 W input. From the comparison made earlier, taking into account that the silicon filter restricted the pumping range of YAG:Ho^{3+}, the threshold of YIG:Ho^{3+} would have been expected to be ~150 W. A reduction of threshold experiment[17] revealed that the 500-W lamp provides only 60% of the power required for cw operation of our best crystal.

Failure to achieve cw oscillation is attributed to residual losses in most of the flux grown crystals. Pulse

[15] We are greatly indebted to Dr. F. K. Reinhart and J. J. Schott for applying the antireflection coatings.

[16] Coatings were applied by Lambda Optics, Berkeley Heights, N. J.

[17] L. F. Johnson, G. D. Boyd, K. Nassau, and R. R. Soden, Phys. Rev. 126, 1406 (1962).

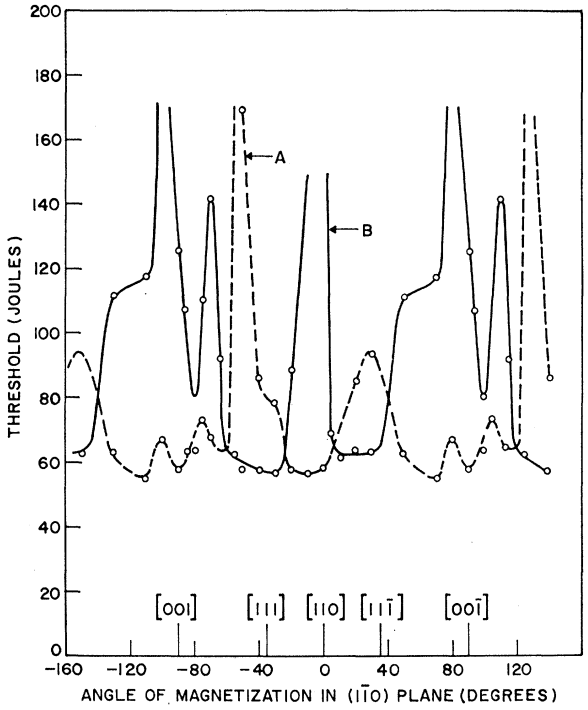

FIG. 11. Variation of threshold of maser lines A and B as the magnetization is rotated in the (1$\bar{1}$0) plane.

threshold measurements as a function of mirror reflectivity reveal an internal loss of typically 5% per cm in crystals grown in large crucibles (yielding maser rods >1 in. long). Losses are lower in crystals grown in smaller crucibles but crystal size is also smaller ($\sim\frac{1}{4}$ in.). Spectrographic analysis failed to reveal a distinction between the two. Absorption measurements on the maser materials and on YIG crystals doped with the possibly troublesome rare-earth impurities Tb^{3+}, Eu^{3+}, Sm^{3+}, and Pr^{3+} also failed to indicate a significant level of absorption at 2.1 μ. However, flux inclusions and other such defects are invariably present in these crystals and, despite efforts to avoid these regions by visual inspection or with the aid of an infrared image converter, it is felt that the presence of these or other such scattering defects probably accounts for the losses observed.

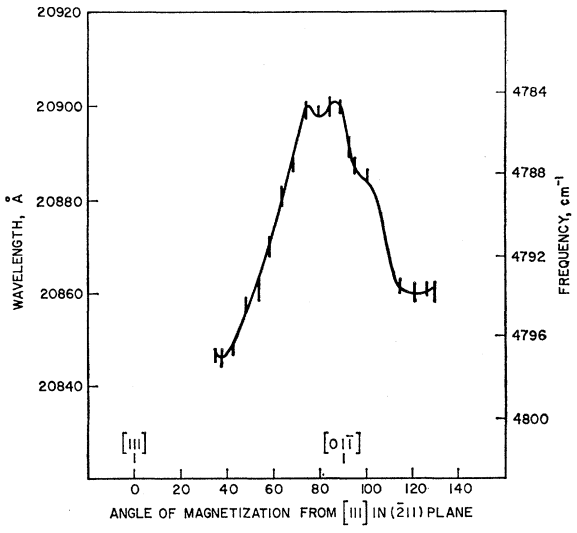

FIG. 12. Wavelength variation of strongest emission peak of Ho^{3+} in YIG at 77°K as the magnetization is rotated in the (2$\bar{1}$1) plane.

C. Magnetic Tuning of Coherent Emission from Ho^{3+} in YIG

Due to the ferrimagnetic nature of YIG there are a number of magneto-optical effects which may be exploited to substantially influence the coherent output of YIG:Ho^{3+}. For example, (1) frequency modulation and tuning is possible through the anisotropic shifting of the Ho^{3+} energy levels in the combined crystal and exchange fields; (2) amplitude modulation may be effected by varying the angle between the magnetization and the direction of light propagation[18,19]; (3) the state of polarization of the light beam may be altered by varying the direction of the magnetization.[19] To the present time, we have investigated only the first of these, and the results are described next.

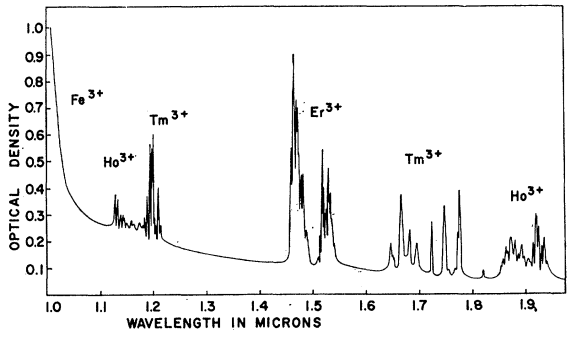

FIG. 13. Absorption spectrum at 77°K of YIG containing 5% Er^{3+}, 5% Tm^{3+}, and 2% Ho^{3+} ions. Crystal thickness 1.6 mm.

Magnetic tuning was carried out with a cylindrical rod whose axis coincided with a ⟨110⟩ crystal direction. The rod was rotated about its axis normal to a magnetic field of 2800 G, causing the magnetization **M** to be swept through directions in a {110} plane. The tuning observed at about 85°K for the two maser lines of lowest threshold is shown in Fig. 10. The arrows pointing to the wavelength scale indicate the wavelengths of the maser lines with no external magnetic field. It will be noted that these wavelengths are identical to those observed when the field is applied in the [111] direction, as they should be since the spon-

[18] At 77°K, YIG exhibits a magnetic rotation of 140°/cm at 2.09 μ when the magnetization is parallel to the direction of propagation (Ref. 3).

[19] C. G. B. Garrett, IEEE J. Quantum Electron. **QE-3**, 139 (1967).

taneous magnetization lies along ⟨111⟩ with no external field.

Tuning extends over a range of about 70 Å (16 cm^{-1}) from 2.0842 to 2.0912 μ. On the steepest portion of the tuning curves, the slope is about 1 cm^{-1}/degree rotation. However, no one line is dominant throughout this entire range. Although the threshold of the dominant line (whichever one it may be) remains relatively constant as **M** is rotated, varying between 55 and 75 J, the threshold of each line individually undergoes large excursions (Fig. 11). For instance, as **M** is rotated from [110] towards [00$\bar{1}$], line A has the lower threshold to about 5° from [110], then line B dominates to about 40°, and then line A again throughout the remaining interval. There is no great change in threshold of the dominant line because the fluorescence giving rise to maser oscillation consists principally of emission from only one type of site, irrespective of the direction of **M**. This can be seen in the magnetic anisotropy data (Fig. 7) in the failure to observe splittings in the region

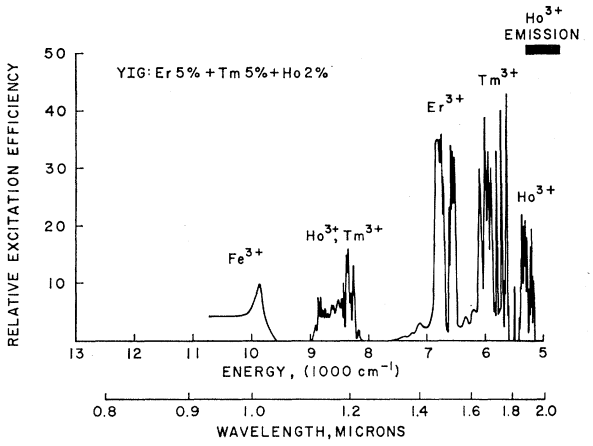

FIG. 14. The 77°K excitation spectrum for ${}^5I_7 \rightarrow {}^5I_8$ emission from Ho^{3+} in YIG containing 5% Er^{3+}, 5% Tm^{3+}, and 2% Ho^{3+}.

of the maser transitions as **M** departs from [111]. The excursions in threshold of the individual lines are primarily a consequence of the shifting of the two overlapping transitions (making up a given maser line) into and out of coincidence as the magnetization is rotated. The departure of the curves in Figs. 10 and 11 from perfect mirror symmetry about the [110] direction is attributed to a slight misorientation of the crystal.

The magnetic tuning of the maser output shown in Fig. 10 represents frequency changes observed as **M** varies in a {110} plane. Unfortunately, the full tuning range of 70 Å is not spanned by the line of lowest threshold. However, other planes will exhibit different and perhaps more desirable characteristics. Figure 12 shows the wavelength variation of the strongest fluorescence peak at 77°K as **M** is swept in a {211} plane. Over the angular range from about 40°–75° from [111] the peak varies smoothly over an interval of

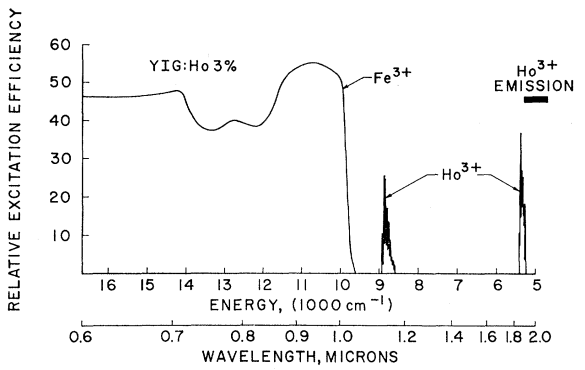

FIG. 15. The 77°K excitation spectrum for Ho^{3+} emission in YIG in which fluorescence emanating from the irradiated front surface is observed.

about 55 Å. Although measurements were not made on a ⟨211⟩ axis maser crystal, it is expected that the wavelength of the maser line of lowest threshold will behave accordingly.

EXCITATION SPECTRA AND ENERGY TRANSFER

Earlier work with diamagnetic yttrium aluminum garnet has shown that highly efficient coherent emission from Ho^{3+} ions is obtained with the aid of energy transfer from Er^{3+} and Tm^{3+} ions.[6] Similarly, a comparison of the absorption spectrum of YIG containing Er^{3+}, Tm^{3+}, and Ho^{3+} ions (Fig. 13) with the excitation spectrum for Ho^{3+} emission (Fig. 14) reveals $Er^{3+} \rightarrow Ho^{3+}$ and $Tm^{3+} \rightarrow Ho^{3+}$ energy transfer, with transfer efficiencies close to unity. In addition, fluorescence from Ho^{3+} is also weakly excited by Fe^{3+} absorption near 1 μ. Since the Fe^{3+} absorption depth decreases rapidly with decreasing wavelength, the effect is more pronounced when fluorescence emanating from the irradiated front surface is observed (Fig. 15), and shows that Fe^{3+} absorption in the visible and near infrared provides broad-pump bands for Ho^{3+} emission at 2 μ.

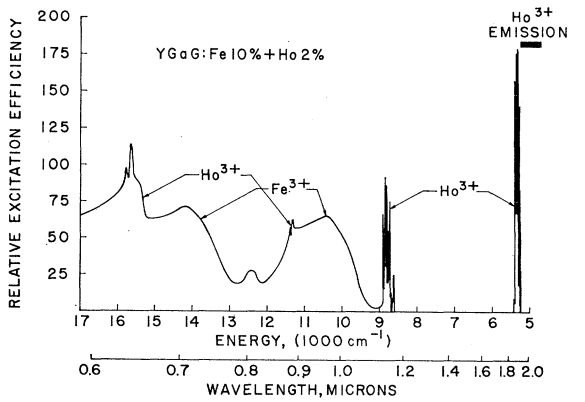

FIG. 16. The excitation spectrum for Ho^{3+} emission at 77°K in YGaG: Fe^{3+} (10%)+Ho^{3+} (2%).

The effectiveness of $Fe^{3+} \rightarrow Ho^{3+}$ energy transfer is more readily determined if the Fe^{3+} content is reduced. Comparison of the absorption and Ho^{3+} excitation spectra for YGaG containing 10% Fe and 2% Ho shows that the fluorescence quantum efficiency is near unity when exciting the Fe^{3+} absorption band centered at 0.9 μ (Fig. 16). The efficiency is also high for the band at 0.7 μ, but this band is obscured in absorption by an overlapping band due to an unknown defect. However, these efficiencies cannot be maintained in YIG due to excess Fe^{3+} absorption near the surface. Therefore, for fluorescence studies at low temperature or cw maser experiments, radiation below 1 μ must be rejected.

ACKNOWLEDGMENTS

We are pleased to acknowledge many helpful discussions with Dr. C. G. B. Garrett. We also express our appreciation to C. R. Radice, Jr., C. R. Staton, and R. A. Thomas for experimental assistance, Miss D. M. Dodd for zero-field absorption data, and E. M. Kelly for assistance with the growth of crystals.

PHYSICAL REVIEW B VOLUME 1, NUMBER 5 1 MARCH 1970

Spin Relaxation of Cr^{3+} in MgO: Evidence for Localized Modes*

R. L. HARTMAN AND J. S. BENNETT
Physical Sciences Laboratory, Redstone Arsenal, Alabama 35809

AND

J. G. CASTLE, JR.
University of Alabama in Huntsville, Alabama 35807

(Received 31 October 1969)

Measurements of the relaxation of Cr^{3+} spins in cubic sites in MgO have been extended by fast pulsed saturation up to 180 K and by line broadening from 130 to 430 K. Explanations based on harmonic lattice vibrations must be modified to account for an observed linear dependence of $1/T_1$ on T above 350 K. The relaxation is accurately given over seven decades of T_1 by $1/T_1 = AT + F(n) + B\,\mathrm{csch}(\Delta/T)$, where $A = 0.93$ $\mathrm{sec^{-1}\,K^{-1}}$, $B = 1.20 \times 10^7$ $\mathrm{sec^{-1}}$, $\Delta = 537 \pm 5$ K. The expected Raman relaxation function $F(n)$ accounts for more than 50% of the relaxation only between 30 and 40 K, and could have the usual form $T^n J_{n-1}$ with $n = 5$ or 7. Apparently, motions localized around each Cr^{3+} ion dominate the ground-state relaxation. The csch function suggests relaxation via localized modes having temperature-independent amplitudes. The localized mode frequencies coincide with a high-density region found in the vibronic sideband of the R line of Cr^{3+} in MgO.

I. INTRODUCTION

THE possibility of introducing inaccuracies into calculations of spin relaxation time by use of harmonic phonon spectra was pointed out by Van Vleck[1] in a discussion on chrome alum: "Conceivably the oscillations most active in modulating the cluster $Cr \cdot 6H_2O$ are not typical of the crystal as a whole and have a different distribution law." A theoretical description of localized vibrational modes in crystals was given soon after that by Lifshitz.[2] Effects of localized vibrations have been observed in a variety of ways, including spin relaxation,[3,4] optical spectra,[5] infrared absorption,[6] and Raman scattering of laser light.[7] The pertinent vibrations have been discussed recently by Maradudin[8] in terms of three classes: localized modes, gap modes, and resonance modes. We find it necessary to consider effects of localized vibrations in order to explain the temperature dependence of the spin relaxation of Cr^{3+} in MgO.

The purpose of this paper is to report rather extensive observations of spin relaxation of Cr^{3+} in cubic sites in MgO. We offer an interpretation which accurately fits all the data and in retrospect seems simpler than the usual calculation of complete lattice sums.[1,4] The model attributes almost all of the observable relaxation above 40 K to a narrow frequency band of localized vibrations. Initial measurements[9] of the relaxation time T_1 for temperatures up to 100 K indicated discrepancies in the predictions of relaxation via Raman scattering.

* Partially supported by U. S. Army Research Office (Durham).

[1] J. H. Van Vleck, Phys. Rev. **57**, 426 (1940); in *Spin-Lattice Relaxation in Ionic Solids*, edited by A. A. Manenkov and R. Orbach (Harper and Row Publishers, Inc., New York, 1966), p. 46.

[2] I. M. Lifshitz, J. Phys. USSR **7**, 215 (1943); **7**, 249 (1943); **8**, 89 (1944).

[3] D. W. Feldman, J. G. Castle, Jr., and G. R. Wagner, Phy- Rev. **145**, 237 (1966).

[4] J. G. Castle, Jr., in *Localized Excitations in Solids*, edited b- R. F. Wallis (Plenum Press, Inc., New York, 1968), p. 386.

[5] M. D. Sturge, in *Solid State Physics*, edited by F. Seitz, D. Turnbull, and H. Ehrenreich (Academic Press Inc., New York, 1967), Vol. 20, p. 91.

[6] R. E. Shamu, W. M. Hartmann, and E. L. Yasaitis, Phys. Rev. **170**, 822 (1968).

[7] D. W. Feldman, M. Ashkin, and J. H. Parker, Phys. Rev. Letters **17**, 1209 (1966).

[8] A. A. Maradudin, in *Localized Excitations in Solids*, edited by R. F. Wallis (Plenum Press, Inc., New York, 1968), p. 1.

[9] J. G. Castle, Jr., D. W. Feldman, and P. G. Klemens, in *Advances in Quantum Electronics* (Columbia University Press, New York, 1961), p. 414.